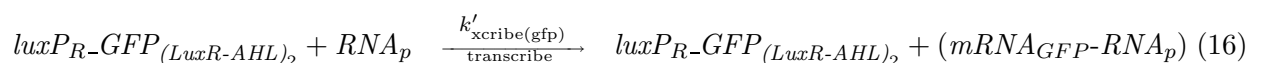
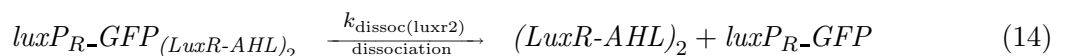
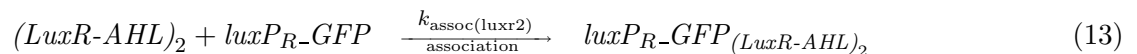
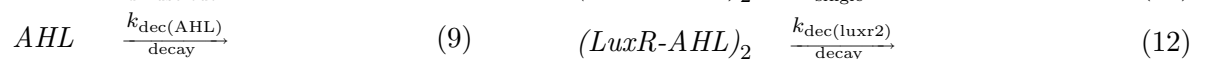
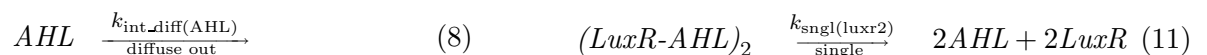
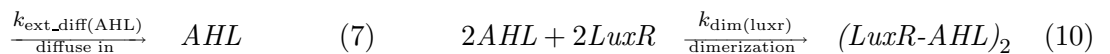
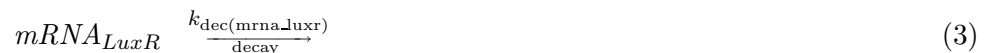
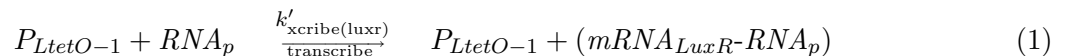


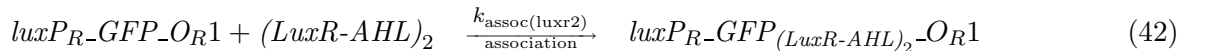
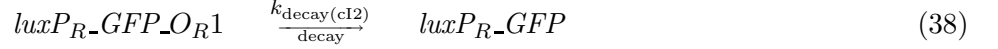
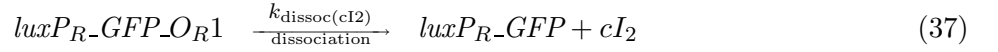
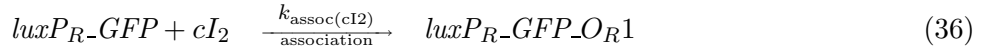
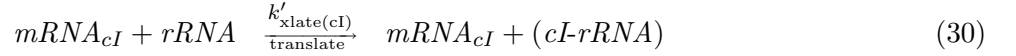
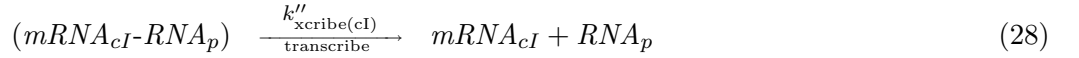
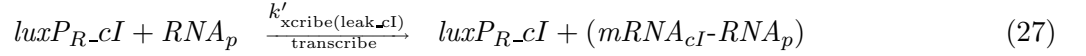
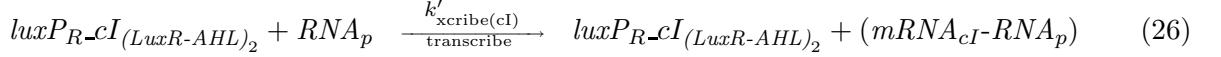
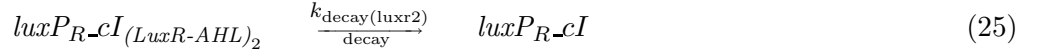
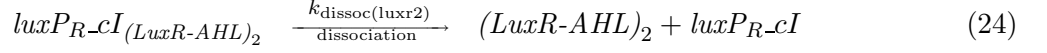
Supporting Text

Modeling and Simulations

The design of the pulse-generating network began with mathematical models of genetic regulatory mechanisms. These mechanisms included transcriptional control, mRNA transcripts, repression through cooperative binding, translation of mRNA, acyl-homoserine lactone (AHL) diffusion, and degradation of proteins. These simulations enabled us to analyze system behavior and to determine which experimental parameters should be adjusted to optimize the performance of the system.

Deterministic Modeling. The pulse-generating network was described by 23 molecular species and 44 chemical reactions. Consequently, the system was modeled by 23 continuous-time differential equations with 44 kinetic rates. Below is a description of all biochemical reactions that were modeled.





The values of the kinetic parameters used in the simulations were initially obtained from the literature and educated guesses (1). Because many of the *in vivo* rates of the biochemical reactions we simulated are unknown, we performed a “best-fit” kinetic parameter search on a subset of the parameters, including the transcription, translation, and decay of CI and GFP. The first step involved simulating the response of the system to five different input concentrations with 1,000 sets of randomly chosen parameter values. We found five sets of values that matched our experimental observations of GFP fluorescence from Fig. 3. Out of these five different sets of values, only one set matched the observed behavior of the circuit shown in Fig. 4b. These rates were subsequently used for the analysis in the paper (Table 1). The dynamic behavior of the system was simulated by solving the differential equations using MATLAB’s stiff differential equation solver ode15s. This solver is a variable order solver based on the numerical differential formulas that optionally uses backward differential formulas (Gear’s method).

Plasmids. Fig. 6 shows the sender plasmid pLuxI-Tet8 that encodes an AHL synthase (LuxI) under the control of the promoter PLtetO-1. The transcription of LuxI is terminated by the terminator T1. It contains a chloramphenicol marker [Cm(r)] and a ColE1 replication origin. The plasmid also has another terminator T0 between Cm(r) and ColE1 genes.

The pulse-generator circuit is composed of two plasmids, namely pLTSUB-202-RBSH and pPSSUB-101-mut4 shown in Fig. 6. pLTSUB-202-RBSH encodes CI(LVA), a destabilized version of the CI repressor, and enhanced cyan fluorescent protein (ECFP) under the control of luxP_R (ECFP is not used in the current study). This bicistronic construct includes a separate ribosome-binding site (RBS H) for CI(LVA) gene and RBSII for ECFP gene. This plasmid also contains constitutive expression of LuxR under the control of luxP_L. It has T1 terminator after ECFP gene, T0 terminator after Kan(r) gene, and rrnBT1 terminator after LuxR gene. CI(LVA) was destabilized with a 12-aa *ssrA* tag. pLTSUB-202-RBSH contains a kanamycin resistance marker and a p15A replication origin.

The other plasmid pPSSUB-101-mut4 contains a destabilized version of GFP (GFP(LVA)) under the control of a novel hybrid promoter luxP_RCI-O_R1 that consists of the wild-type luxP_R promoter with a CI O_R1 operator site inserted at the +1 transcription start (Fig. 7). It contains a chloramphenicol marker and a ColE1 replication origin. This plasmid has T0 terminator after Cm(r) gene. pPSSUB-101-mut4 is a variant of pPSSUB-101 with a single base C → A mutation in the fourth base of O_R1 to reduce repressor/operator affinity.

Experiments

Liquid-Phase Experiments Sample FACS Data. Fig. 8 reports typical FACS population statistics of the pulse response (140 nM AHL induction on pLTSUB-202-RBSH/pPSSUB-101-mut4 is shown). The histograms reveal that the distribution of GFP intensities was relatively tight during the pulse rise, whereas the distribution was wider during the pulse falling phase.

Solid-Phase Experiments. Fig. 9 shows the time series fluorescence of individual pulse-generating cells on the M9 agar slide at four different positions from the senders. On average, for each position there were 345 cells in the field of view in the beginning and 525 cells at the end. For positions 1-5, 67.5%, 19.8%, 4.9%, 1.3%, and 0.0% of the cells respectively exhibited a detectable pulse. There were wide variations in the amplitudes of the pulses among the different cells. The variations were greater in the solid-phase than in the liquid-phase experiments, likely

because of the increased heterogeneity in the environmental conditions. Specifically, the noise in the diffusion of AHL molecules likely plays a significant role in the variations, as well as differences in nutrient conditions.

A time-lapse movie of the pulse generator at cropped portions from each of the five different positions is published as Movie 1. Please make sure to view the movie with the Quicktime viewer as other movie viewers are not able to display it properly.

1. Weiss, R., Basu, S., Kalmbach, A., Hooshangi, S., Karig, D., Mehreja, R. & Netravali, I. (2003) *Nat. Comput.* **2**, 47-84.